JOURNAL OF SPACECRAFT AND ROCKETS
Vol. 38, No. 1, January–February 2001

Numerical Analysis of Convection/Transpiration Cooling

David E. Glass,* Arthur D. Dilley,† and H. Neale Kelly‡
Analytical Services and Materials, Inc., Hampton, Virginia 23666

An innovative concept utilizing the natural porosity of refractory-composite materials and hydrogen coolant to provide convective and transpiration cooling and oxidation protection has been numerically studied for surfaces exposed to a high-heat-flux, high-temperature environment such as hypersonic vehicle engine combustor walls. A boundary-layer code and a porous media finite difference code were utilized to analyze the effect of convection and transpiration cooling on surface heat flux and temperature. The boundary-layer code determined that transpiration flow is able to provide blocking of the surface heat flux only if it is above a minimum level due to heat addition from combustion of the hydrogen transpirant. The porous media analysis indicated that cooling of the surface is attained with coolant flow rates that are in the same range as those required for blocking.

Nomenclature

a	=	coefficient in Nu
B_0	=	coefficient for first-order effect in permeability, in.^{2}
b	=	coefficient in Nu
Cp_c	=	coolant specific heat, Btu/lbm · °F
D_h	=	hydraulic diameter of the coolant channel, in.
d	=	coefficient in finite difference equation
G	=	mass flow rate per unit area, lbm/in.^{2} · s
h	=	heat transfer coefficient, Btu/in. · s · °F or Btu/in.^{3} · s · °F
i	=	spacial index in finite difference equation
K	=	permeability, in.^{2}/s
K_0	=	coefficient for second-order effect in permeability, in.
k	=	thermal conductivity, Btu/in. · s · °F
L	=	thickness of porous media, in.
M	=	molecular weight, mol
m	=	molecular mass, kg/molecule
Nu	=	Nusselt number
P	=	pressure, psi
Pr	=	Prandtl number
q_{appl}	=	applied heat flux at combustor wall, Btu/ft^2 · s
Re	=	Reynolds number
R_{H2}	=	hydrogen gas constant, Btu/lbm · °F
R_u	=	universal gas constant, Btu/lbm · mol · °R
T	=	temperature, °F
V	=	velocity of coolant, in./s
x	=	spacial coordinate in porous media, in.
ΔP	=	pressure difference ($P_{\mathrm{ch}} - P_{\mathrm{comb}}$), psi
ε	=	porosity
κ	=	Boltzmann constant, J/molecule · K
μ	=	viscosity, lbm/in. · s
ρ	=	density, lbm/in.^{3}

Subscripts

avg	=	average
c	=	coolant in porous media
ch	=	coolant in coolant channel
comb	=	combustion chamber
eff	=	effective
m	=	porous media
s	=	surface
v	=	volumetric, in porous media
wall	=	conditions at surface of combustor wall

Presented as Paper 99-4911 at the 9th International Space Planes and Hypersonic Systems and Technologies Conference, Norfolk, VA, 1–5 November 1999; received 3 March 2000; revision received 9 August 2000; accepted for publication 13 August 2000.

*Senior Engineer; currently Aerospace Engineer, NASA Langley Research Center, MS 396, Hampton, VA 23681. Associate Fellow AIAA.

†Research Engineer; currently Senior Engineer, Swales Aerospace, MS 353X, NASA Langley Research Center, Hampton, VA 23681.

‡Senior Engineer; currently retired.

Introduction

DESIGN and trade studies of hypersonic vehicles have shown significant benefits for operation at high engine wall and coolant/fuel temperatures. One approach to achieving these operational conditions in engine combustors has led to the development of a platinum-clad Mo-50Re alloy for the convectively cooled structure. This approach was taken due to the requirements for a material with both high-temperature stability and high thermal conductivity to accommodate the anticipated high heat fluxes. However, these materials are expensive, and because Mo-Re has poor oxidation resistance, serious problems can result from exposure to oxygen should a breach occur in the cladding.

Cooled refractory composites have been considered for nozzles, but have not been proposed for combustors because of their relatively low thermal conductivity. Furthermore, use of convectively cooled refractory composites incorporating leak-tight metallic liners in the coolant passage and oxidation protection surface coatings causes additional design constraints. These constraints are due to material incompatibility and thermal expansion differences between the tubes and the liners, as well as the external coating compatibility with the combustor environment.

An innovative concept utilizing the natural porosity of refractory-composite materials and hydrogen coolant to provide convective and transpiration (CONTRAN) cooling and oxidation protection has been proposed for surfaces exposed to a high-heat-flux, high-temperature environment such as hypersonic vehicle engine combustor walls. The concept relies on the hydrogen coolant to permeate the selectively densified refractory-composite material such as carbon/carbon (C/C) to provide a reliable cooling and oxidation protection system. The CONTRAN concept shown in Fig. 1 is based on the fundamental premise that the natural porosity of refractory-composite materials leads to leaks. Though little can be done to completely eliminate the leaks, the leak rate can be controlled through selective densification of the refractory-composite materials. The hydrogen coolant that permeates the C/C prevents oxidation, and the transpiring coolant also significantly reduces the heat flux. Because transpiration is very effective in cooling the structure and blocks some heat input exterior to the surface, the very high thermal conductivity requirements imposed by a pure convective cooling system are relaxed. Similarly, the needs for impermeable oxidation protection coatings and leak-free coolant liners are eliminated. An important aspect of the CONTRAN concept is control of the spatial variation of the hydrogen permeability through the composite, both to minimize the coolant leakage out of the back side and to accommodate the variations in the heating conditions over the hot surface.

A comparison of coolant weight for a convection and transpiration cooling system is illustrated in Fig. 2. The particular example shown

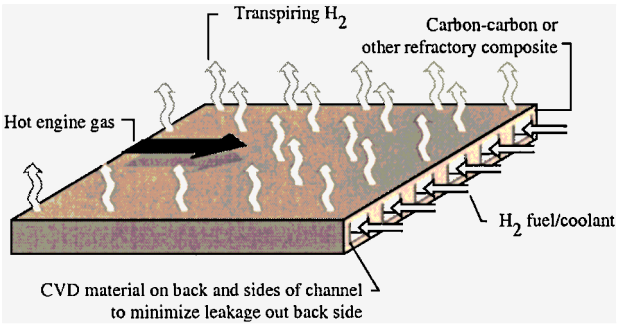

Fig. 1 CONTRAN cooling concept.

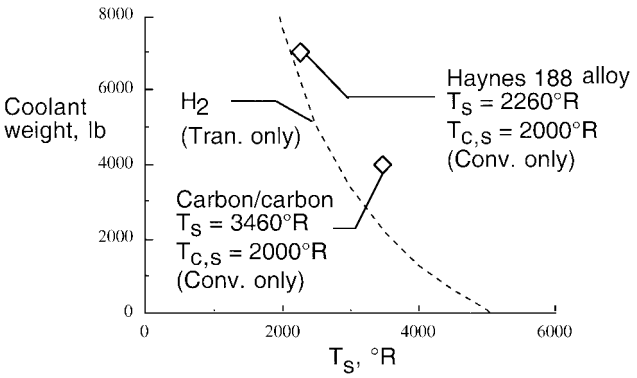

Fig. 2 Inlet closure door coolant weight as a function of surface temperature for hydrogen coolant.

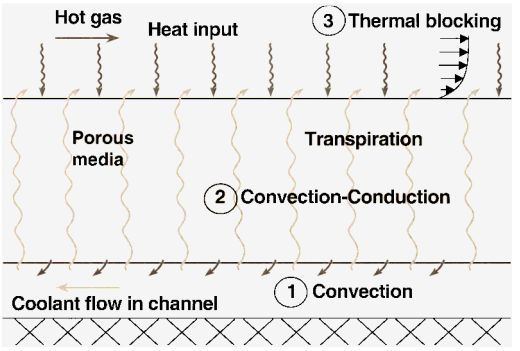

Fig. 3 Schematic diagram showing aspects of CONTRAN cooling.

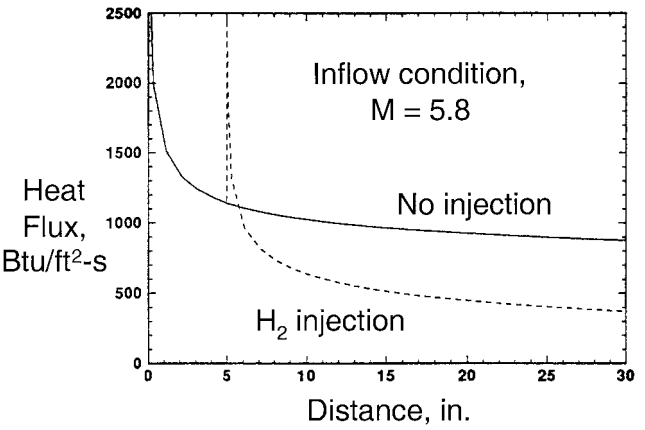

Fig. 4 Heat-transfer rates on a flat plate with and without transpiration cooling.

is for an inlet closure door, not a combustor wall panel, and the cooling mode is pure transpiration (with an energy balance for which wall surface temperature equals outlet coolant temperature), which is a limiting case of the CONTRAN concept. The heat blocking effects of transpiration cooling are not considered. The closure door is used during reentry to prevent hot gases from entering the engine, and the expendable coolant, which is dumped overboard, represents a direct weight penalty. The dashed line in Fig. 2 illustrates the reduction in coolant weight penalty as a function of hot surface temperature where the coolant temperature is permitted to rise to the surface temperature, as will occur with transpiration cooling. If a surface can tolerate ~5000°R, no weight penalty is incurred because no coolant is required. Previous engine design studies, as shown by the two design conditions (symbols), indicate that the coolant weight penalty can be reduced by ~3000 lb by switching from the baseline Haynes 188 alloy door to a C/C door. However, the C/C design is constrained by the 3460°R limit imposed by the oxidation protection coatings and the 2000°R limit imposed by metallic tube liners. For the C/C design, an additional 2000-lb savings can be realized with transpiration cooling (as shown on the dashed line) by the elimination of the 2000°R limit for the coolant tubes.

Transpiration cooling systems have been proposed for engine cowl lips and other stagnation regions. However, there has been concern about the transpiring coolant altering the effective aerodynamic shape of the components, the potential impact of combustion on the inlet and overall engine performance, the potential detrimental effects of shock impingement on transpiration cooling effectiveness, and the unknown effects of combustion of the transpirant on the cooling process. The last two of these concerns are addressed numerically in this study. No quantitative experimental validation on the effectiveness of CONTRAN cooling in C/C exists in the literature. However, an unpublished experimental effort accompanying this study did qualitatively validate the effectiveness of the concept. Follow-on experimental studies would be required to validate the numerical results presented here.

The numerical analysis results presented utilized two codes to model the CONTRAN cooling of C/C. A boundary-layer code was used to calculate the effect of the transpiration cooling on the surface heat flux (effect 1 in Fig. 3). A porous media code modeled both the convective cooling in the coolant channel and the thermal-fluid mechanics of transpiration in the porous media, as illustrated by effects 2 and 3 in Fig. 3. The two codes were used to numerically demonstrate the feasibility of using CONTRAN cooling for scramjet engine combustors.

Boundary-Layer Analysis

The viscous flow along the C/C surface was computed using an implicit finite difference boundary-layer code.[1] Heat transfer predictions with this code have been favorably compared with numerous hypersonic flat-plate experimental data sets. Either a perfect gas or a reacting mixture of perfect gases in chemical equilibrium can be computed. The chemical equilibrium capability was previously used to study real-gas effects on hypersonic boundary-layer stability.[2] Experimental studies performed at General Applied Science Laboratories, Ronkonkoma, New York, have generated trends similar to those of the boundary-layer analysis presented here.[3]

In the present equilibrium chemistry analysis, a binary diffusion model is assumed with injection of the hydrogen coolant into the freestream gas. The species composition of the gas mixture is determined using a Gibbs free-energy minimization procedure. The external flowfield was modeled as a flat plate with either a constant or varying pressure at the boundary-layer edge. Injection of coolant occurred some distance downstream of the leading edge of the flat plate to permit injection into a developed turbulent boundary layer. The heat transfer predicted by the code included both the combustion and the blocking effect of the hydrogen coolant. In all cases, the boundary layer remained attached. Elimination or removal of freestream oxygen at the surface resulted from burning of the oxygen and transpiring hydrogen.

Figure 4 shows the heat-transfer rates with and without hydrogen transpiration. The inflow conditions for this case (Mach 5.8) are based on flight-scale scramjet combustor conditions. The geometry was a flat plate, and a turbulent boundary layer was developed before injection begins. The coolant injection rate was 0.04% of the freestream mass flow rate. The spike in the heat transfer with injection was caused by the immediate burning of the hydrogen coolant

and surface oxygen when injection starts. After the oxygen near the surface was eliminated by burning with hydrogen, the heating rate drops below the no-injection case. This result demonstrates the blockage effect of the hydrogen transpiration.

The boundary-layer code was also used to simulate hydrogen transpiration into a scramjet combustor flowfield with pressure gradients to simulate shockwaves. The geometry was a flat plate, representing the constant area section of a scramjet combustor. The inflow condition (Mach 4.22) was determined from a pulse facility that is used to test subscale scramjet designs. The shockwave was modeled by varying the pressure at the boundary-layer edge. Heat transfer results from a parametric study of the injection rates are shown in Fig. 5. The highest injection rate was 0.28% of the freestream mass flow rate. Injection rates above this level separated the turbulent boundary layer, and no solution was available from the boundary-layer code. A sharp increase in pressure occurs at approximately 9 in., with a smaller increase at approximately 13.5 in. Injection of hydrogen into the fully turbulent boundary layer starts slightly ahead of the first shock impingement. At the lowest injection level, 0.08% of the freestream mass flow rate, the heat transfer to the surface had actually increased due to the hydrogen injection. As the injection rate increased, the heat transfer was reduced below the no-injection case.

The reason for the increase in heat transfer at low injection levels is shown in Fig. 6. Figure 6 shows the axial variation of the oxygen concentration at the surface. At the lowest injection level, the oxygen was not eliminated from the surface and injected hydrogen continued to burn near the surface. The burning resulted in increased heating rates. At the highest injection level, the oxygen was rapidly removed from the surface and the heating rates decreased. In this case, the

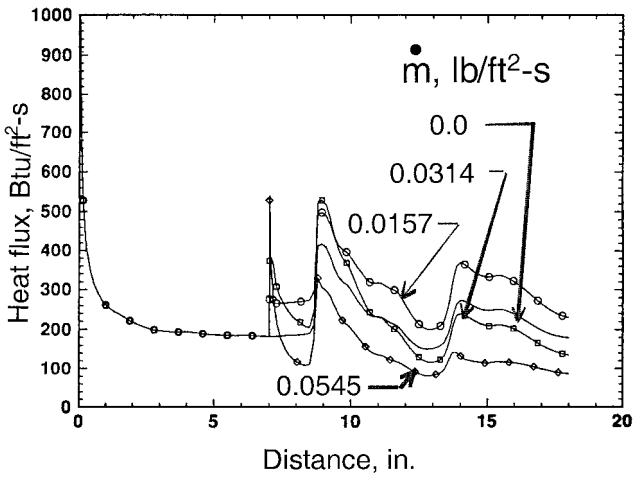

Fig. 5 Effect of hydrogen mass flow rate on the surface heat flux with a pressure gradient.

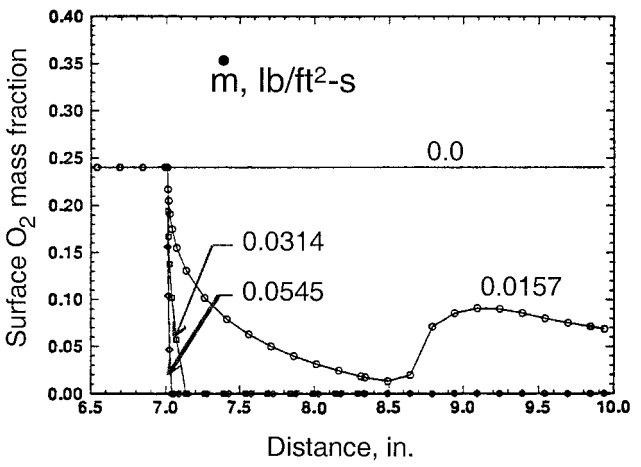

Fig. 6 Effect of hydrogen mass flow rate on the oxygen concentration at the surface.

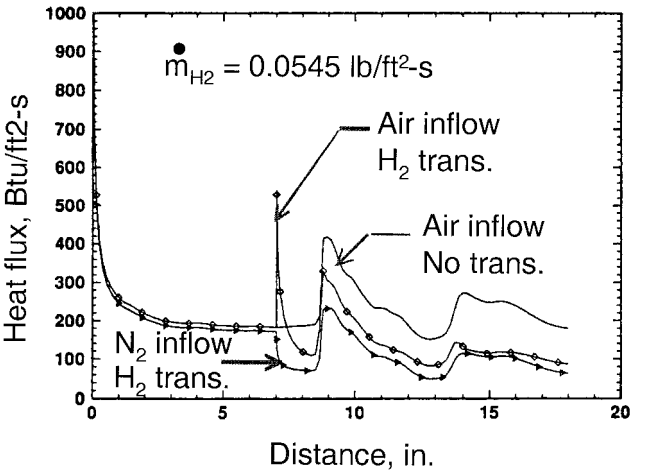

Fig. 7 Effect of inflow gas on the surface heat flux.

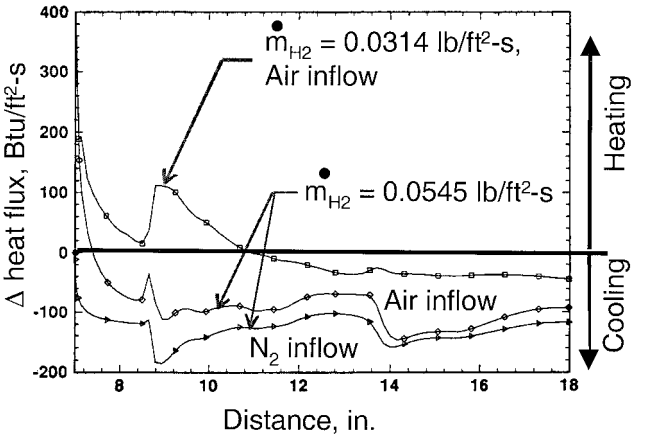

Fig. 8 Blockage effect of the gas injection on the surface heat flux.

burning of the hydrogen occurred away from the surface and the expected reduction in heat transfer from transpiration cooling was realized.

The effect of combustion of transpirant on heat transfer was observed by changing the composition of the inflow gas. The heating rates for air and pure nitrogen are shown in Fig. 7. The nitrogen inflow case does not have a spike in the heat transfer immediately following the start of injection because of the absence of oxygen. In this case, the heat transfer drops immediately after the injection begins. After the first shock impingement, the results with the nitrogen inflow are slightly below the air inflow case.

The blockage effect of the hydrogen injection is shown in Fig. 8. In Fig. 8, the difference in heating rate due to injection is plotted for several cases considered in this study. Thus, negative heat flux indicates cooling and positive heat flux indicates additional heating. The effects of nitrogen inflow and increased injection rates are clearly shown. The boundary-layer code results indicate that pressure gradients due to the shocks do not remove the transpiration flow from the surface, thus reducing the cooling. Instead, with the highest injection rates, the region where the shocks impinge experience a significant cooling effect of the transpiration flow. These results confirm the ability of the CONTRAN concept to provide thermal and oxidation protection using hydrogen transpiration through a porous medium. They also indicate the importance of injection rate in removing the freestream oxygen at the surface to facilitate the reduction in heat transfer. If larger injection rates, separating the incoming boundary layer, are required, a Navier–Stokes analysis method must be used.

Porous Media Analysis

The approach taken in the porous media analysis was to solve three coupled differential equations for the C/C temperature, the

hydrogen temperature, and the hydrogen pressure in the porous media. A general convection boundary condition was assumed at both boundaries of the porous media, that is, inside the coolant channel and at the combustor surface. At the combustor wall surface, blocking (a reduction) of the applied heat flux occurred due to the injection of the hydrogen into the boundary layer. The permeability and mass flux were calculated in the code. A one-dimensional analysis was utilized because lateral conduction is relatively small. (A set of two-dimensional transient equations for heat and mass transfer in a porous media can be found in Ref. 4.) The analysis was performed at both the combustor entrance and exit, thus accounting for the significant difference in boundary conditions at the two locations. A discussion of the procedure used for solving the three equations for the three unknowns (T_m, T_c, and P) as well as the porous media (C/C) permeability and the coolant (hydrogen) mass flux follows.

Porous Media Temperatures and Coolant Temperatures and Pressures

The first step was to calculate the porous media temperature, coolant temperature, and coolant pressure. These calculations required the solution of three differential equations for three variables, T_m, T_c, and P. A schematic diagram of the porous media with the channel coolant flow rate, temperature, and pressure is shown in Fig. 9.

A one-dimensional energy balance for the porous media results in the following equation:

$$\frac{\mathrm{d}^2 T_m}{\mathrm{d}x^2} - \frac{h_v}{k_{\text{eff}}}(T_m - T_c) = 0 \tag{1}$$

where k_{eff} is considered by treating the porous media as a porous solid with no coolant.

The volumetric heat transfer coefficient h_v is calculated according to an empirical formula for flow in a porous media and has units of British thermal units per cubic inch second degree Rankine. The porous media flow Nusselt number is defined by Florio et al.[5,6] as

$$Nu_v = aRe^b \tag{2}$$

where $a = 2.22 \times 10^{-6}$ and $b = 0.703$ and where both were experimentally determined for argon gas in charred composites. The Reynolds number Re is defined as

$$Re = -\frac{\rho_c B_0^{1.5}}{\mu_c^2 \varepsilon}\frac{\mathrm{d}P}{\mathrm{d}x} \tag{3}$$

The pressure of the coolant in the porous media is the second variable that must be obtained, and it is determined from the solution of a first-order differential equation given by

$$-\frac{\mathrm{d}P}{\mathrm{d}x} = \frac{\mu_c G_c}{\rho_c B_0} \tag{4}$$

where the viscosity and density are functions of temperature and pressure.

Once Nu_v is calculated, h_v is obtained from

$$h_v = Nu_v k_c / B_0 \tag{5}$$

The volumetric heat transfer coefficient h_v was calculated at each node as a function of temperature.

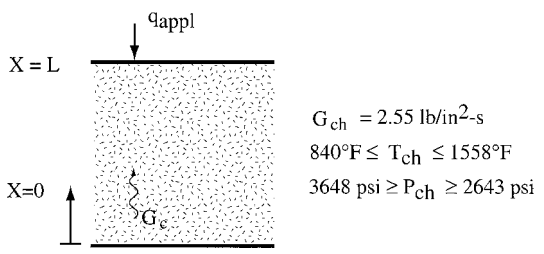

Fig. 9 Schematic diagram of the porous media and channel coolant values used in thermal analysis.

The boundary conditions are given as

$$h_{\text{ch}}(T_{\text{ch}} - T_m) = -k_{\text{eff}}\frac{\mathrm{d}T_m}{\mathrm{d}x} \tag{6a}$$

at $x = 0$ and

$$q_{\text{appl}} = -k_{\text{eff}}\frac{\mathrm{d}T_m}{\mathrm{d}x} \tag{6b}$$

at $x = L$.

The coolant heat transfer coefficient h_{ch} was calculated from the Nusselt number for turbulent flow. The coolant channel Nusselt number is defined as[7]

$$Nu_{\text{ch}} = 0.027 Re^{\frac{4}{5}} Pr^{\frac{1}{3}} [\mu_{\text{ch}}/\mu_s]^{\frac{1}{4}} \tag{7}$$

Additional analytical correlations for convective heat transfer for hydrogen can be found in the literature.[8]

Once the Nusselt number was calculated, the coolant heat transfer coefficient was obtained from

$$h_{\text{ch}} = Nu_{\text{ch}} k_c / D_h \tag{8}$$

where D_h is the hydraulic diameter of the coolant channel.

The third differential equation to be solved [with the other two solving for the porous media temperature, Eq. (1), and coolant pressure, Eq. (4)] provides the coolant temperature distribution. An energy balance on the coolant yields

$$\frac{\mathrm{d}T_c}{\mathrm{d}x} - \frac{h_v}{G_c \mathrm{Cp}_c}(T_m - T_c) = 0 \tag{9}$$

where Cp_c is the coolant specific heat. The remaining boundary condition that was used is that the coolant temperature at $x = 0$ equals the temperature of the coolant in the channel, $T_c(0) = T_{\text{ch}}$. The coolant and porous media temperatures are coupled and must be solved simultaneously. The coolant temperature can be solved explicitly, with the coolant temperature in finite difference form being

$$T_{c,i} = (d\Delta x T_{m,i} + T_{c,i-1})/(1 + d\Delta x) \tag{10}$$

where

$$d = h_v / G_c \mathrm{Cp}_c \tag{11}$$

and i is the nodal index that increases with x.

The three sets of equations were solved using finite differences. Gaussian elimination was used to solve the system of equations for the porous media temperatures. Convergence occurred when the difference between successive temperatures divided by the new temperature was less than 1×10^{-4} at each node. A grid convergence study was also performed to determine the sensitivity of the numerical results to grid spacing.

Permeability

The permeability K is a function of both temperature and pressure and is defined as

$$K = B_0 P_{\text{avg}}/\mu_{\text{avg}} + \tfrac{4}{3} K_0 V_{\text{avg}} \tag{12}$$

The coefficients K_0 (4.094×10^{-8} in.) and B_0 (4.96×10^{-13} in.^{2}) are constants that are determined when obtaining the permeability as a function of temperature and pressure. The values used here were obtained from unpublished data for C/C resulting from work performed by Oak Ridge National Laboratory for NASA Langley Research Center. The average dynamic viscosity μ_{avg} (1.039×10^{-6} lbm/in. · s) is defined to be the viscosity at the average temperature $T_{\text{avg}} = 1300$°F.

The average pressure in the porous media is defined as

$$P_{\text{avg}} = (P_{\text{ch}} + P_{\text{comb}})/2 \tag{13}$$

The average velocity in the porous media is defined as

$$V_{\text{avg}} = \sqrt{3\kappa T_{\text{avg}}/m} \tag{14}$$

where κ is the Boltzmann constant (1.3803×10^{-23} J/molecule · K) and m is the molecular mass (3.34522×10^{-27} kg/molecule).

Mass Flux

The mass flow rate per unit area G_c can be calculated using an equation originally proposed in Ref. 9:

$$G_c = (K \Delta P / L)(M / R_u T_{\text{avg}}) \tag{15}$$

This expression requires the average temperature of the porous media and the pressure difference between the coolant channel and the combustor. The differential equation used earlier to calculate the coolant pressure in the porous media uses the mass flux calculated here, along with temperature and pressure dependent coolant properties throughout the porous media.

The porous media temperatures were solved using finite differences and were then used to calculate the coolant temperatures and pressures. The coolant temperatures and pressures were then used to recalculate the porous media temperatures until convergence was reached.

Porous Media Results

A parametric study was performed using the finite difference code described to evaluate the effect of the transpiration mass flow rate (which is a function of permeability and pressure) and heat flux on the surface temperature of the heated surface. The C/C thermal conductivity and the hydrogen coolant viscosity and thermal conductivity are temperature dependent and are calculated at each node. The hydrogen coolant specific heat and density are both pressure and temperature dependent. The convection coefficient in the channel was calculated numerically, and the channel was assumed to have a square cross section 0.1×0.1 in. with a mass flux of 2.55 lb/in.^{2} · s. The thickness of the porous media L was assumed to be 0.1 in. Because the coolant in the coolant channel was heated along the flow path, two different coolant temperatures were used, 840 and 1560°F. The temperatures represent the inlet and outlet coolant temperatures for a typical combustor. The corresponding coolant pressures were 3648 and 2643 psi, respectively. These coolant temperatures and pressures are representative of pure convection cooling. The convection coefficient for the coolant in the porous media was also calculated numerically. In this analysis, the surface temperature is allowed to reach a value dependent on all of the conditions of the problem. The applied heat flux is specified, but the surface temperature and transpiration flux are calculated.

In Fig. 10, the surface temperature of the C/C is plotted as a function of the transpiration mass flux and the applied surface heat flux for the conditions at the entrance of the coolant channel, with the channel coolant at a temperature of 840°F and a pressure of 3648 psi. The surface heat flux is assumed to include any blocking effect of the transpiring coolant. The porous media analysis does not calculate the magnitude of the blocking effect of the transpiration but utilizes the net heat flux applied to the surface (which could be calculated by the boundary-layer code). The surface temperature was calculated

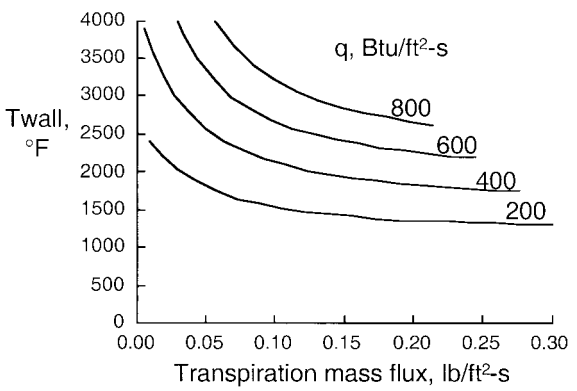

Fig. 10 Combustion wall surface temperature as a function of transpiration mass flux and applied surface heat flux at the entrance to the coolant channel (coolant at 840°F and 3648 psi).

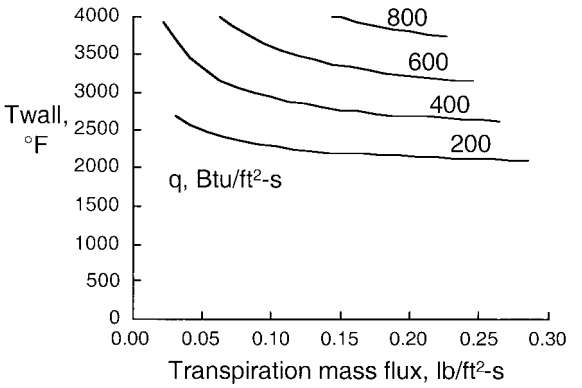

Fig. 11 Combustion wall surface temperature as a function of transpiration mass flux and applied surface heat flux at the coolant exit to the combustor (coolant at 1558°F and 2643 psi).

for four different heat fluxes, ranging from 200 to 800 Btu/ft^2 · s. The mass flux is a function of the pressure, temperature, and permeability. Because the pressures and temperatures were determined as part of the analysis, only the permeability needed to be varied to obtain the range of mass fluxes G_c. The permeability was changed by varying the coefficients B_0 and K_0. The porosity and effective thermal conductivity of the porous media were not modified in this analysis. (Note that h_v is also a strong function of mass flux and permeability.) From Fig. 10, it can be seen that as the mass flux is increased to higher levels, the surface temperature appears to become less sensitive to transpiration mass flux, indicating that for high flow rates, the wall surface temperature essentially becomes a function of applied heat flux only.

In Fig. 11, the surface temperature of the C/C is plotted as a function of the transpiration mass flux and the applied surface heat flux for the conditions at the exit of the coolant channel, with the channel coolant at a temperature of 1558°F and a coolant pressure of 2643 psi. Again, the surface temperature is calculated for four different heat fluxes, ranging from 200 to 800 Btu/ft^2 · s. From Fig. 11, it can again be seen that as the mass flux is increased, the surface temperature appears to become less sensitive to mass flow rate. Here, the wall surface temperatures are higher than for the entrance conditions, due to both the higher coolant temperature and the lower pressure, which results in a lower mass flux for a given permeability.

The results from Figs. 10 and 11 indicate that C/C permeabilities that result in transpiration fluxes greater than 0.25 lb/ft^2 · s result in little further reduction of surface temperature at the given heat flux levels. The transpiration mass fluxes used for blocking in the boundary-layer analysis were up to 0.0545 lb/ft^2 · s. The mass fluxes required to reduce (block) the heat flux at the surface (calculated from the boundary-layer analysis) are, therefore, at levels where the wall temperature is sensitive to mass flux variations. The small transpiration heat flux in the boundary-layer analysis, $<1\%$ of the freestream mass flux, is, thus, in the region where it has a significant reduction on the surface temperature.

Though the numerical analysis has indicated that CONTRAN cooling C/C is feasible, several issues would arise before its actual implementation. It is imperative that positive flow of the transpiring fluid be maintained. Flow blockage or inflow of hot combustion gases could be catastrophic. The analytical studies that verified that oxidizing gases could be prevented from reaching the C/C surface indicated that the effects of hydrogen injection at low flow rates was detrimental to heat transfer (because of combustion in the boundary layer), but produced favorable blocking effects at higher flow rates. Especially important was that the analysis indicated that impinging shocks did not remove the blocking effectiveness. Perhaps the most critical technical obstacle that must be overcome is the interaction of hot hydrogen with C/C that was encountered during the unpublished experimental tests that were part of this study. These interactions were evidenced by micrographs of tested specimens and changing electrical and flow performance during testing. The micrographs indicated severe erosion of specimens exposed to hot hydrogen and little or no damage to specimens exposed to nitrogen at corresponding test conditions. Even though it may be

possible to reduce the reaction rate of the hydrogen with the C/C by several different methods, due to the large surface area resulting from the porosity, any technique must be adequately experimentally verified.

Summary

A convection/transpiration cooling technique for cooling engine combustors was numerically studied by using both a boundary-layer code and a porous media analysis. The boundary-layer analysis determined that transpiration cooling can block the heat flux from the combustor. The porous media analysis indicated that values of the surface temperatures are reached where increases in the coolant flow rate (controlled by permeability) have little further cooling effect on the surface temperature. The boundary-layer and porous media analysis could be coupled to further investigate the feasibility of this convection/transpiration cooling technique for hypersonic vehicle combustor walls.

Acknowledgments

The authors greatly appreciate the support of the U.S. Air Force Research Laboratory at Wright–Patterson Air Force Base, Ohio, for support of this work under a Phase I SBIR, Contract F33657-93C-2227. The assistance of Clay Anderson of NASA Langley Research Center in running the boundary-layer code is greatly appreciated.

References

[1]Anderson, E. C., and Lewis, C. H., "Laminar or Turbulent Boundary-Layer Flows of Perfect Gases or Reacting Gas Mixtures in Chemical Equilibrium," NASA CR-1893, May 1971.

[2]Malik, M. R., and Anderson, E. C., "Real Gas Effects on Hypersonic Boundary-Layer Stability," *Physics of Fluids*, Vol. 3, No. 5, 1991, pp. 803–821.

[3]Bakos, R., and Calleja, J., "Experimental Investigation of Transpiration Cooling in a Hypervelocity Combustor," General Applied Science Labs., GASL TR-364, Ronkonkoma, NY, Jan. 1995.

[4]Curry, D. M., and Cox, J. E., "The Effect of the Porous Materials Characteristics on the Internal Heat and Mass Transfer," American Society of Mechanical Engineers, Paper 73-HT-49, 1973.

[5]Florio, J., Jr., Henderson, J. B., Test, F. L., and Hariharan, R., "A Study of the Effects of the Assumption of Local-Thermal Equilibrium on the Overall Thermal-Induced Response of a Decomposing, Glass-Filled Polymer Composite," *International Journal of Heat and Mass Transfer*, Vol. 34, No. 1, 1991, pp. 135–147.

[6]Florio, J., Jr., Henderson, J. B., Test, F. L., and Hariharan, R., "Experimental Determination of Volumetric Heat Transfer Coefficients in Decomposing Polymer Composite," *ASME Winter Annual Meeting*, Heat Transfer Div. Vol. 117, American Society of Mechanical Engineers, Fairfield, NJ, 1989, pp. 51–60.

[7]Incropera, F. P., and DeWitt, D. P., *Fundamentals of Heat and Mass Transfer*, 3rd ed., Wiley, New York, 1990, p. 496.

[8]Dziedzic, W. M., Jones, S. C., Gould, D. C., and Petley, D. H., "An Analytical Comparison of Convective Heat Transfer Correlations in Supercritical Hydrogen," AIAA Paper 91-1382, June 1991.

[9]Grove, D. M., *Porous Carbon Solids*, edited by R. L. Bond, Academic Press, New York, 1967, pp. 155–201.

M. Torres
Associate Editor